Effect of the Dispersion of Organic Rectorite on the Nonisothermal Crystallization Kinetics and Melting Behaviors of Nylon 6 Nanocomposites

Shaojie Yue, Wei Gong, Ning Qi, Bo Wang, Wei Zhou, Yuchan Zhu

Department of Physics, Wuhan University, Wuhan, 430072, China

Received 8 April 2008; accepted 17 June 2008
DOI 10.1002/app.28847
Published online 8 September 2008 in Wiley InterScience (www.interscience.wiley.com).

ABSTRACT: The effects of the dispersion of organic rectorite (OREC) and the cooling rate on the crystallization behavior of nylon 6/OREC nanocomposites have been systematically investigated with X-ray diffraction, transmission electron microscopy, differential scanning calorimetry, and the modified Ozawa model. Some important parameters have been calculated, including the crystallization half-time, crystallization peak temperature, and relative crystallinity. Experimental results indicate that the crystallization rate of the nylon 6/OREC nanocomposites is faster than that of nylon 6 at a given cooling rate, and the difference in the values of the Ozawa exponent for nylon 6 and nylon 6/OREC nanocomposites reveals tridimensional growth with heterogeneous nucleation. The analysis of the Ozawa exponent m has suggested that the better the dispersion of OREC is, the more suitable it will be for the formation of spherulitic growth. On the other hand, in analyses of the melting behavior, we have found an unusual phenomenon: the lower the cooling rate is, the more favorable it is for the formation of the γ form. Our experimental results indicate that the dispersion of OREC plays an important role in determining the crystallization behavior of nylon 6/OREC nanocomposites. © 2008 Wiley Periodicals, Inc. J Appl Polym Sci 110: 3149–3155, 2008

Key words: crystallization; kinetics (polym.); nanocomposites

INTRODUCTION

Polymer/layered-silicate nanocomposites have been widely investigated because they frequently exhibit unexpected hybrid properties synergistically derived from the two components.[1–10] Recently, much attention has been focused on the crystallization behavior of polymers in the presence of nanolayered clays because the addition of nanoscale clays can change the crystallization kinetics, the crystalline morphology, and the crystal forms.

Many factors can affect the crystallization behavior of polymers, such as the chain conformation near the interface, the activation barrier to nucleation, and the chain mobility. The addition of an inorganic clay to polymeric matrices further increases the complexity of this phenomenon. Different results have been reported about the observed effects of nanoclay fillers on the crystallization behavior of polymers. Homminga et at.[11] showed that the dispersed silicate layers act as impurities and reduce the overall crystallization kinetics of polyamide 6 (PA-6). Opposite results were observed by Fornes and Paul,[12] who found that bulk polymer crystallization kinetics can be significantly increased for PA-6 nanocomposites. Although extensive research efforts have been devoted to the effect of clay on the crystallization of nylon 6 nanocomposites, the influence of nanofillers on the crystallization behaviors of nylon 6 nanocomposites is being further studied.

Another crystallization effect of inorganic nanosized silicate layers is that a filler can promote the growth of a specific crystalline form that is not favorable in the neat polymer. The incorporation of clay can promote the growth of the γ form of nylon 6/clay nanocomposites, whereas the neat polymer tends to crystallize in the α form.[13] The crystallization behavior of PA-6/montmorillonite nanocomposites and the role of the silicate layers have been addressed as well.[3,6,10–12,14–18] Such studies are very complicated because of the unusual crystallization behavior of neat PA-6 itself. For example, crystalline PA-6 displays different polymorphic structures, particularly the monoclinic α and pseudohexagonal γ forms, and their relative amounts are influenced by the presence of silicate layers.

Comprehensive investigations are challenging because of the sensitivity of nucleation and growth

Correspondence to: B. Wang (bwang@positron.whu.edu.cn).

Contract grant sponsor: National Natural Science Foundation of China.
Contract grant sponsor: Center of Nanoscience and Nanotechnology Research of Wuhan University.

to the process history and the lack of sufficiently quantitative techniques to describe nanofiller morphology (dispersion, orientation, and local concentration). As mentioned previously, the crystallization behavior of nanocomposites needs to be further investigated. In this work, a detailed examination of the crystallization behavior of nylon 6/organic rectorite (OREC) nanocomposites was performed, including the effects of the cooling rate, organoclay concentration, dispersion of OREC, and melting behavior.

EXPERIMENTAL

Materials and sample preparation

PA-6 and rectorite were supplied by Yueyang Petrochemical Co. (Yueyang, China) and Hubei Celebrities Technology Co. (Wuhan, China), respectively. The exchange cation of rectorite is Ca^{2+}, and the cation exchange capacity used in this study was 44.9 mequiv/100 g. Hexadecylamine was manufactured by Schuchardt Co. (Munich, Germany). The organically modified rectorite was made by a cation exchange reaction between rectorite and hexadecylamine salt. The nylon 6/OREC nanocomposites NCN1 (OREC concentration = 1 wt %) and NCN5 (OREC concentration = 5 wt %) were successfully prepared by melt mixing with a twin-screw extruder (Nanjing Giant Co., Nanjing, China; screw diameter = 30 mm, length-to-diameter ratio = 42).

Morphological characterization

X-ray diffraction (XRD) was performed with Cu Kα radiation (λ = 0.15406 nm) at a voltage of 40 kV and a current of 50 mA. The XRD patterns were recorded with a step size of 0.02° from 2θ = 0.7° to 2θ = 10°. XRD analysis was used to measure the change in the interlayer spacing of clays on the basis of Bragg's law. The degree of dispersion of OREC was studied with transmission electron microscopy (TEM) with a Hitachi (Naka, Japan) H-7600 at an operating voltage of 100 kV.

Differential scanning calorimetry (DSC) procedures

The nonisothermal analyses were carried out with a PerkinElmer (Shanghai, China) DSC-7 differential scanning calorimeter thermal analyzer. About 4 mg of the polymer samples was used for DSC measurements.

The following nonisothermal crystallization runs were conducted: (1) as-cast samples were heated from 45 to 250°C at a heating rate of 10°C/min; (2) they were held for 10 min to completely eliminate the heating history; (3) the samples were cooled to 45°C at four different cooling rates of 5, 10, 20, and 40°C/min; and (4) then the samples were secondarily heated to 250°C at the same heating rate of 10°C/min. The thermograms corresponding to the heating and cooling cycles were recorded and analyzed to estimate the nonisothermal crystallization kinetics and the degree of crystallinity.

RESULTS AND DISCUSSION

Morphological analyses

Figure 1 shows XRD patterns for the pristine OREC and the nanocomposites containing different OREC concentrations. The OREC pattern reveals an intense peak around 2θ = 2.46°, corresponding to a basal spacing of 3.57 nm. The XRD pattern of NCN1 does not show a characteristic basal reflection, which is indicative of exfoliated structures. However, the NCN5 pattern reveals a low, broad shallow peak around 2θ = 1.8° corresponding to a spacing of 4.90 nm. This result suggests the formation of intercalated nanocomposites.

TEM photomicrographs of nanocomposites, shown in Figure 2, provide a better representation of the composite structures. The NCN1 image, shown in Figure 2(a), reveals well-exfoliated structures. In Figure 2(b), intercalated structures can be observed in the nylon 6 matrix. These observations are in agreement with the XRD results.

Nonisothermal crystallization behavior

The crystallization exotherms of neat nylon 6 and nylon 6/OREC nanocomposites for nonisothermal crystallization from the melt at four different cooling rates are shown in Figure 3. From Figure 3, some useful parameters, such as the crystallization peak

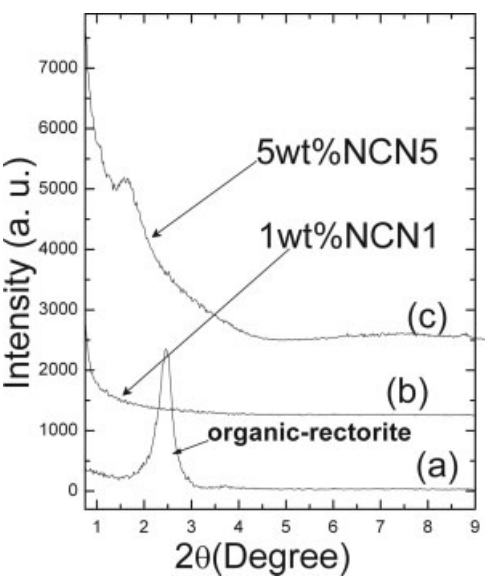

Figure 1 XRD patterns of (a) OREC and the nanocomposites with OREC loadings of (b) 1 and (c) 5 wt %.

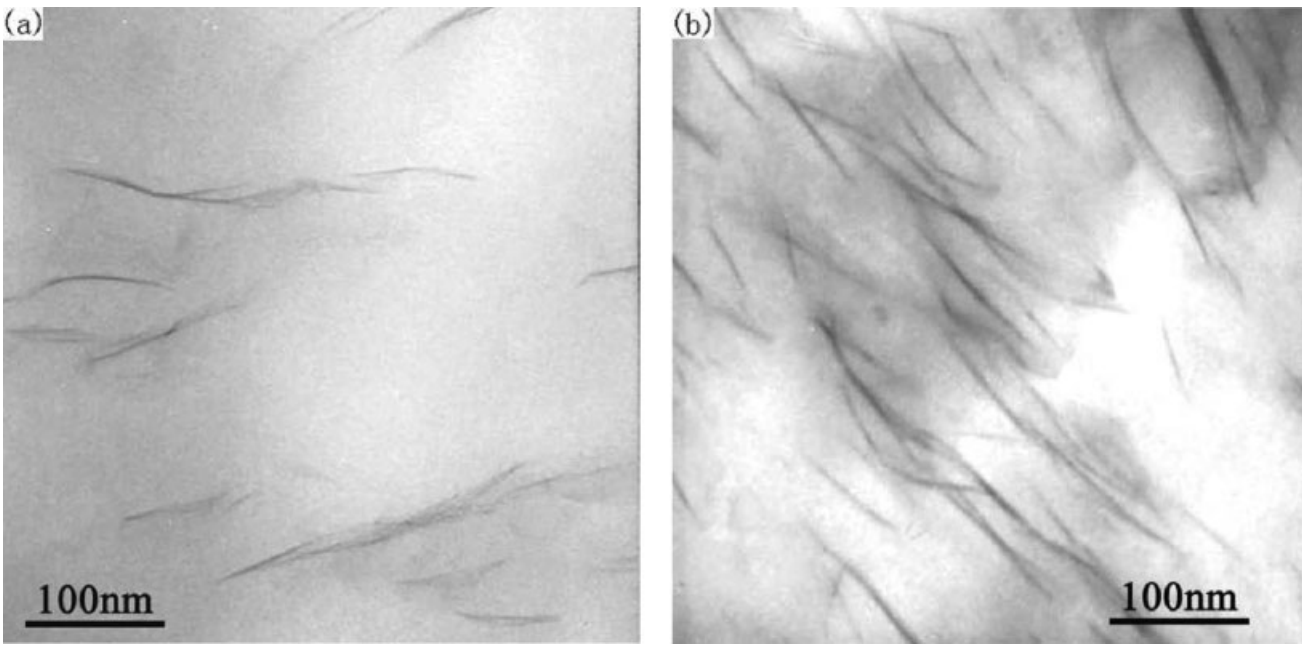

Figure 2 Bright-field TEM images of the nanocomposites: (a) NCN1 and (b) NCN5.

temperature (T_p), full width at half-maximum (fwhm), initial crystallization temperature (T_i), the difference between the initial temperature and the crystallization peak temperature [ΔT ($\Delta T = T_p - T_i$)], and initial slope of the exothermic peak at a high temperature (S_i), can be obtained, as shown in Table I. From this table, we can see the following. First, with an increasing cooling rate for both nylon 6 and nylon 6/OREC nanocomposites, T_p shifts, as expected, to a lower temperature, and the exothermic peak is widened (fwhm becomes larger). This fact indicates that the higher the cooling rate is, the higher the overcooling is of the system. Thus, the segmental chain motion becomes restricted, and this leads to a reduction in crystal perfection and the formation of a wider peak.[19] Second, for a given cooling rate, T_p values of nylon 6/OREC nanocomposites are higher than those of neat nylon 6, and this indicates that OREC, added to nylon 6, acts as an effective nucleating agent and increases the rate of crystallization of nylon 6. Third, at the same cooling rate, the values of S_i increase with the OREC concentration increasing, and this means that OREC is a good nucleating agent and results in an increase in the crystallization rate of nylon 6, which can be related to the decrease in ΔT ($\Delta T = T_p - T_i$), except at the cooling rate of 40k/min.

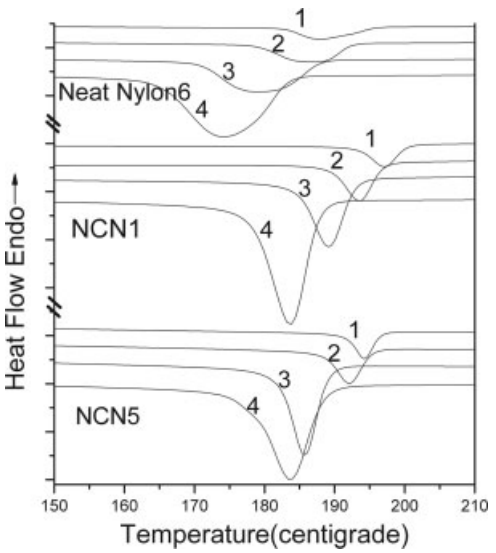

Figure 3 Nonisothermal melt crystallization exotherms of neat nylon 6, NCN1, and NCN5 at four different cooling rates: (1) 5, (2) 10, (3) 20, and (4) 40 K/min.

The relative crystallinity [$X(T)$] as a function of the crystallization temperature (T) can be formulated as follows:[20]

TABLE I
Values of S_i, fwhm, T_p, T_i, and ΔT for the Crystallization of Nylon 6 and the Nylon 6/OREC Nanocomposites

Sample	ϕ (°C/min)	S_i	fwhm (°C)	T_p (°C)	T_i (°C)	ΔT
Neat nylon 6	5	0.29	6.65	187.8	195.5	7.7
	10	0.97	7.24	186.0	192.8	6.8
	20	1.04	9.36	179.2	188.8	9.6
	40	1.71	9.61	173.9	184.3	10.4
NCN1	5	1.56	3.56	197.0	201.2	4.2
	10	2.18	3.80	193.6	199.0	5.4
	20	3.19	4.22	189.9	196.6	6.7
	40	5.28	4.91	183.9	190.8	6.9
NCN5	5	2.59	2.64	194.2	197.5	3.3
	10	2.34	3.45	192.1	197.0	4.9
	20	3.45	3.74	185.7	191.2	5.5
	40	6.02	4.09	179.5	192.1	12.6

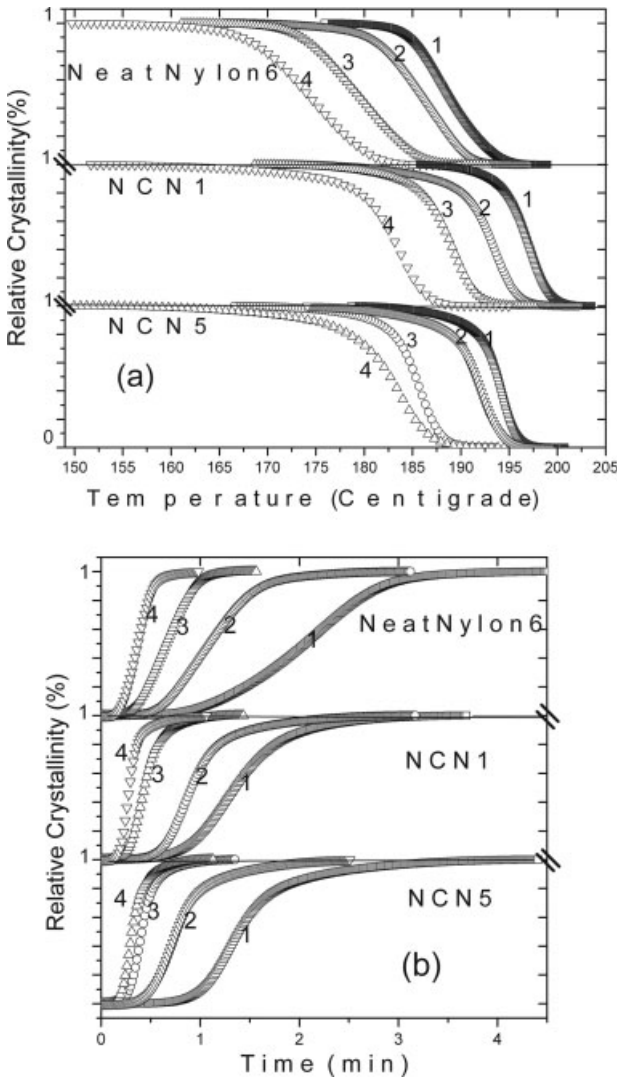

Figure 4 $X(T)$ as a function of the (a) temperature and (b) time of crystallization for nylon 6, NCN1, and NCN5 at four different cooling rates: (1) 5, (2) 10, (3) 20, and (4) 40 K/min.

$$X(T) = \frac{\int_{T_O}^{T} (dH/dT)dT}{\int_{T_O}^{T_E} (dH/dT)dT} \quad (1)$$

where T_O and T_E represent the crystallization onset and end temperatures, respectively, and dH is the enthalpy of crystallization released during the infinitesimal temperature range dT. Figure 4(a) shows the variations of $X(T)$ as a function of temperature for nylon 6 and nylon 6/OREC nanocomposites at various cooling rates. Based on the different cooling rates, the temperature parameter can be converted into a timescale with eq. (2):

$$t = \frac{|T_O - T|}{\phi} \quad (2)$$

where T is the temperature at crystallization time t and ϕ is the cooling (or heating) rate. Plots of the relative degree of crystallinity as a function of time for nylon 6 and nylon 6/OREC nanocomposites are illustrated in Figure 4(b).

An important parameter taken directly from Figure 4(b) is the half-time of crystallization ($t_{1/2}$), which denotes the change in time from the onset of crystallization to the time at which $X(T)$ is 50%. $t_{1/2}$ of the nonisothermal crystallization of all samples is listed in Table II. The higher the cooling rate is, the shorter the time is for completing the crystallization. For a given cooling rate, as expected, the values of $t_{1/2}$ for nanocomposites are shorter than that for neat nylon 6. This fact demonstrates that OREC plays a nucleating role in facilitating crystallization. On the other hand, with increasing OREC content, intercalated and aggregated structures appear and bring about a slight decrease in nucleating agent effects.

Nonisothermal crystallization kinetics based on the Ozawa approach

Because the nonisothermal crystallization is a rate-dependent process, Ozawa[21] took into account the effect of the cooling (or heating) rate on the crystallization process from the melt or glassy state, and on the basis of the observation of the crystallization behavior of PET and PP by Chuah and Gan,[22] the following equations were proposed:

$$\ln[-\ln(1 - X(T))] = \lambda(T - T_\phi) \quad (3)$$

$$T_\phi = \frac{m}{\lambda}\ln\phi + T_1 \quad (4)$$

where T_ϕ is the parameter estimated by equation 3, λ and T_1 are empirical constants and m is the Ozawa exponent, which depends on the dimensions of crystal growth. According to the Ozawa theory, eq. (3) is used only to describe the initial stage of polymer nonisothermal crystallization. For analysis, we chose the nonisothermal crystallization data range of $0.01 < X(T) < 0.40$.

Figure 5 shows the variation of $\ln[-\ln(1 - X(T))]$ versus the temperature. The values of λ and T_ϕ were calculated from the slopes and intercepts of the straight lines. By plotting T_ϕ versus $\ln \phi/\lambda$, we

TABLE II
Values of $t_{1/2}$ for All of the Samples

	$t_{1/2}$ (min)		
ϕ (°C/min)	Neat nylon 6	NCN1	NCN5
5	2.044	1.35	1.39
10	1.098	0.91	0.77
20	0.650	0.44	0.42
40	0.338	0.29	0.28

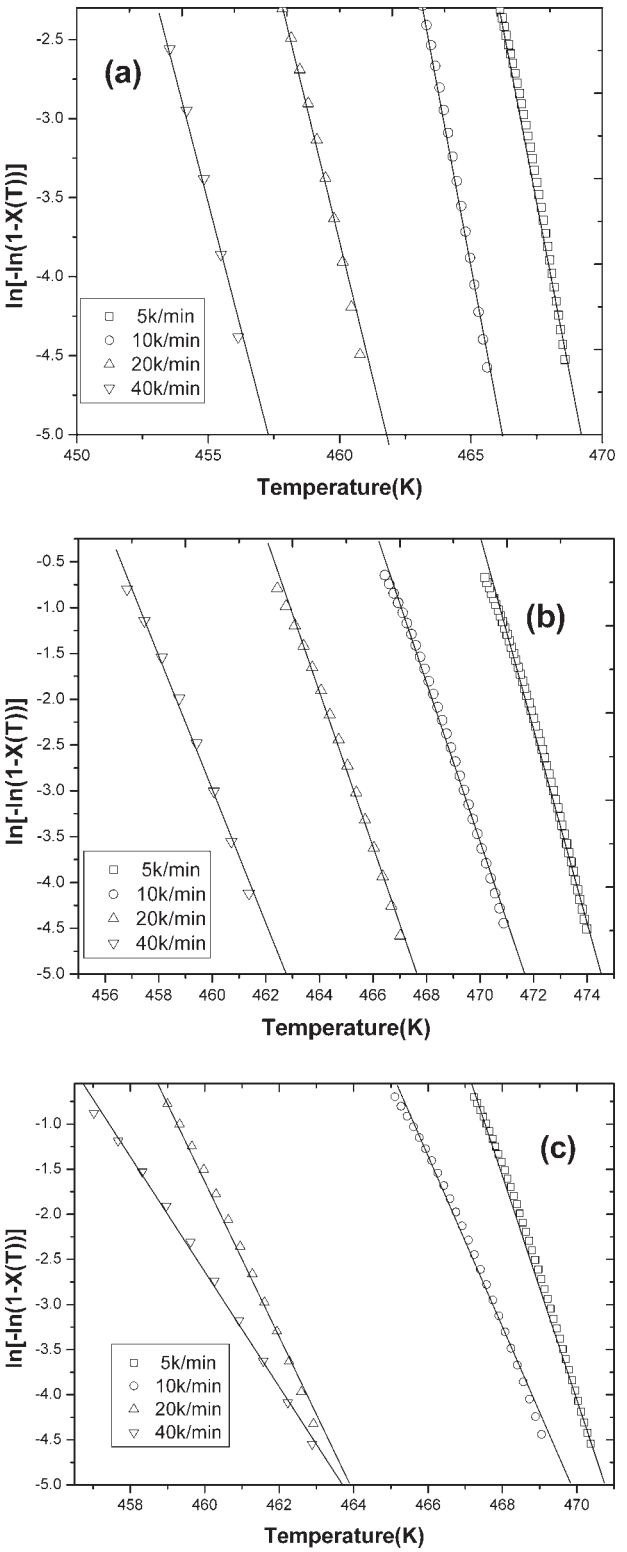

Figure 5 Plots of $\ln\{-\ln[1 - X(T)]\}$ versus the temperature (K) of crystallization for (a) nylon 6, (b) NCN1, and (c) NCN5 at four different cooling rates.

calculated the values of m to be 2.82, 4.51, and 4.10 for neat nylon 6, NCN1, and NCN5, respectively.

It is very clear that the values of m of nylon 6/OREC nanocomposites are higher than that of neat nylon 6, and the maximum appears in sample NCN1, in which OREC is better dispersed overall. Values of m for nylon 6/OREC nanocomposites are indicative of the heterogeneous spherical growth. According to the variations of the m value, we can conclude that spherulitic growth occurs in well-dispersed nylon 6 nanocomposites. The result also means that organoclays act as good nucleating agents.

Melting behavior

Studies of the melting behavior were carried out by secondary heating to 250°C at 10°C/min after cooling to 45°C at four different cooling rates. Figure 6 shows DSC melting endotherms of the samples, and some important parameters are listed in Table III. The crystallinity degree (x_c^c) is calculated as the ratio $\Delta H_m/(1 - \phi)\Delta H_m^o$, where ΔH_m is the apparent enthalpy of crystallization, ΔH_m^o is the extrapolated value of the enthalpy corresponding to the melting of 100% crystalline sample; where ΔH_m^o is 190 J/g[23] and ϕ is the weight fraction of the filler in the nanocomposite.

According to the orientation of the chains, two different kinds of crystalline forms exist in nylon 6, including the γ- and α-crystalline forms, which are related to the different crystalline phases. The effects of OREC on the γ- and α-crystalline forms are shown in Figure 6. It is obvious that each curve contains two endothermic peaks. Low-temperature endothermic peaks can be associated with the γ-crystalline form of nylon 6, as suggested by various researchers.[24–26] High-temperature endothermic

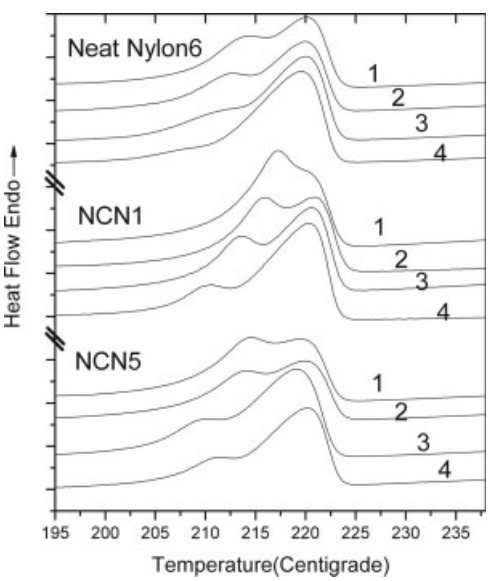

Figure 6 Heating scans of nylon 6, NCN1, and NCN5 at a heating rate of 10 K/min where the previous cooling rates were (1) 5, (2) 10, (3) 20, and (4) 40 K/min.

TABLE III
DSC Data of Nylon 6 and the Nylon 6/OREC Nanocomposites at a Heating Rate of 10K/min

Sample	ϕ (°C/min)	T_m (°C) First	T_m (°C) Second	ΔH^M (J/g)	x_c^c (%)
Neat nylon 6	5	214.31	220.01	59.0	31.05
	10	212.52	219.98	58.0	30.53
	20	211.63	220.04	55.3	29.11
	40	209.56	219.61	51.4	27.05
NCN1	5	217.22	221.01	71.56	38.04
	10	216.12	220.95	69.61	37.01
	20	213.59	220.52	65.74	34.95
	40	210.54	220.25	59.66	31.72
NCN5	5	214.56	219.62	68.83	38.13
	10	214.01	219.93	67.49	37.39
	20	211.75	220.11	59.82	33.14
	40	211.39	220.22	55.43	30.71

peaks around 220°C are attributed to the α-crystalline form. Comparing nylon 6 and nylon 6/OREC nanocomposites with the same heat history, we find that the γ-peak temperatures of the nanocomposites shift to higher temperatures, as shown in Figure 7. Meanwhile, we find that the intensity of the γ peak has a dramatic enhancement, and its width is narrowed. On the other hand, it is obvious that sample NCN1 has the highest crystallization temperature and narrowest peak width, as shown in Figure 7. These results indicate that the better the dispersion is of OREC, the more favorable the formation is of the γ form.

From Figures 7 and 8, we can see that the cooling rate has a marked effect on the crystallization behavior; that is, the degree of crystallinity decreases with the increasing cooling rate at the same OREC content. From Figure 6, it is clear that the lower the cooling rate is, the more favorable it is for the formation of the γ form, and this may stem from the segmental chain relaxation. Our result is in contrast to the results reported by Fornes and Paul,[12] who suggested that rapid cooling forces crystallization at low temperatures at which the rate is limited by polymer chain mobility, and mobility limitations may be the reason for favoring the γ form. Further studies are being conducted regarding this phenomenon.

CONCLUSIONS

The effects of the dispersion of OREC on the crystallization behavior of nylon 6/OREC nanocomposites were systematically investigated. XRD and TEM were employed to characterize the exfoliated and intercalated structures and the dispersion of OREC in nanocomposites. The results revealed that an intercalated morphology (NCN5) and an exfoliated morphology (NCN1) were successfully obtained. Nonisothermal crystallization experiments and analyses were performed with DSC and the modified Ozawa model. We found that the crystallization rate of nylon 6/OREC nanocomposites

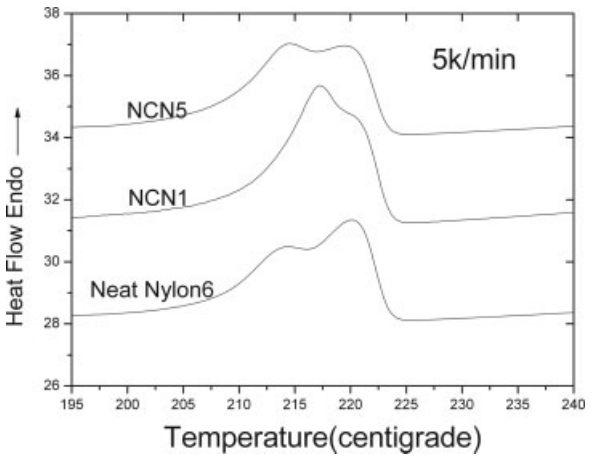

Figure 7 Heat scans of nylon 6, NCN1, and NCN5 at a heating rate of 10 K/min where the previous cooling rate was the same at 5 K/min.

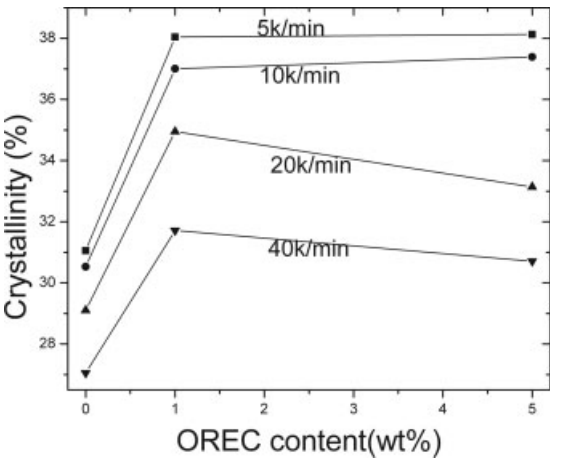

Figure 8 Crystallinity as a function of OREC content at four different cooling rates: (1) 5, (2) 10, (3) 20, and (4) 40 K/min.

is faster than that of nylon 6 at a given cooling rate. The difference in the values of m between neat nylon 6 and nylon 6/OREC nanocomposites suggests that the nonisothermal crystallization of nylon 6/OREC nanocomposites corresponds to tridimensional growth with heterogeneous nucleation.

Melting behaviors of nylon 6 and nylon 6/OREC nanocomposites were also investigated. We found that the addition of OREC favors the formation of the γ form, and x_c^c of nylon 6/OREC nanocomposites increased in comparison with that of neat nylon 6 with the same heat history, especially for NCN1. The results also imply an unusual phenomenon: the lower the cooling rate is, the more favorable it is for the formation of the γ form.

References

1. Messersmith, P. B.; Giannelis, P. Chem Mater 1994, 6, 1719.
2. Messersmith, P. B.; Giannelis, E. P. J Polym Sci Part A: Polym Chem 1995, 33, 1047.
3. Usuki, A.; Kojima, Y.; Kawasumi, M.; Okada, A.; Fukushima, Y.; Kurauchi, T.; Kamigaito, O. J Mater Res 1993, 8, 1179.
4. Yano, K.; Usuki, A.; Kurauchi, T.; Kamigaito, O. J Polym Sci Part A: Polym Chem 1993, 31, 2493.
5. Burnside, S. D.; Giannelis, E. P. Chem Mater 1994, 6, 2216.
6. Vaia, R. A.; Vasudevan, S.; Krawiec, W.; Scanlon, L. G.; Giannelis, E. P. Adv Mater 1995, 7, 154.
7. Aranda, P.; Ruiz-Hitzky, E. Chem Mater 1992, 4, 1395.
8. Wu, J.; Lerner, M. M. Chem Mater 1993, 5, 835.
9. Gilman, J. W. J Appl Clay Sci 1999, 15, 31.
10. Vaia, R. A.; Price, G.; Ruth, P. N.; Nguyen, H. T. J Appl Clay Sci 1999, 15, 67.
11. Homminga, D. S.; Goderis, B.; Vincent, B. F. M.; Gabriel, G. Polymer 2006, 47, 1630.
12. Fornes, T. D.; Paul, D. R. Polymer 2003, 44, 3945.
13. Vahik, K.; Darrin, J. P. Macromolecules 2004, 37, 6480.
14. Wunderlich, B. Macromolecular Physics; Academic: New York, 1976; Vol. 2, Chapter 5.
15. Liu, X.; Wu, Q. Eur Polym J 2002, 38, 1383.
16. Medellin-Rodriguez, F. J.; Burger, C.; Hsiao, B. S.; Chu, B.; Vaia, R. A.; Phillips, S. Polymer 2001, 42, 9015.
17. Lincoln, D. M.; Vaia, R. A.; Wang, Z. G.; Hsiao, B. S.; Krishnamoorti, R. Polymer 2001, 42, 09975.
18. Van, E. S. Ph.D. Thesis, Technical University of Delft, The Netherlands; Chapter 7.
19. Di Lorenzo, M. L.; Silvestre, C. Prog Polym Sci 1999, 24, 917.
20. Cebe, P.; Hong, S. D. Polymer 1986, 27, 1183.
21. Ozawa, T. Polymer 1971, 12, 150.
22. Chuah, K. P.; Gan, S. N. Polymer 1998, 40, 253.
23. Inoue, M. J Polym Sci Part A-2: Polym Phys 1969, 7, 1755.
24. Campoy, I.; Gomez, M. A.; Marco, C. Polymer 1998, 39, 6279.
25. Wu, T. M.; Chen, E. C.; Liao, C. S. Polym Eng Sci 2002, 42, 1141.
26. Liu, X. H.; Wu, Q. J. Polymer 2002, 43, 1933.